

# Analytic Approximation to the GLAP evolution of $F_2(x, Q^2)$ in the small- $x$ region. \*

L. Mankiewicz<sup>†</sup> A. Saalfeld and T. Weigl

*Institut für Theoretische Physik, TU München, Germany*

*October 23, 2018*

## **Abstract:**

We propose a systematic approximation scheme for solving GLAP evolution equations at small Bjorken- $x$ . The approximate solutions interpolate smoothly between hard (singular as  $x^{-(1+\lambda)}$ ,  $\lambda > 0$ ) and soft (singular at most as  $x^{-1}$ ) initial conditions and may be applied in a wide range of  $Q^2$ . The small- $x$  behavior of  $F_2^p(x, Q^2)$  which is extracted from a fit to HERA data agrees with results from a global fit.

---

\*Work supported in part by BMBF

<sup>†</sup>On leave of absence from N. Copernicus Astronomical Center, Polish Academy of Science, ul. Bartycka 18, PL-00-716 Warsaw (Poland)

Understanding the small- $x$  HERA data [1, 2] is nowadays one of the most important challenges to perturbative QCD [3]. In a conventional approach the link between theory and the data is provided by a mathematical parameterization constructed to obey QCD evolution according to Gribov-Lipatov-Altarelli-Parisi (GLAP) equations. Although global fits in the whole  $x$  region play necessarily the most important role [4, 5, 6, 7], many approximations aimed specifically at the small- $x$  region [8, 9, 10, 11] have been proposed with a goal to provide more insight [12] into the otherwise numerically complicated analysis. As it has been emphasized in [13] such an approximate procedure can be justified only if its accuracy with respect to the exact calculation is higher than a typical accuracy of the experimental data. In this letter we present an analysis based on a standard analytical approach to the LO GLAP evolution equations which includes corrections necessary for satisfactory agreement with the state-of-art numerical integration for both hard, (singular as  $x^{-(1+\lambda)}$ ,  $\lambda > 0$ ) and soft (singular at most as  $x^{-1}$ ) initial conditions. By fitting the final formula to the data we can explicitly demonstrate that the analytical approach predicts the same small- $x$  shape of the input distributions as the global fit, as it should be. Our analysis also shows that at  $Q^2$  evolution lengths which are typical for the present data, hard initial conditions may produce significant contributions which possess a similar small- $x$  behavior as those resulting from soft initial conditions. As a consequence, we have found that the same data can be described by either moderately hard  $\lambda \sim 0.2$  or soft initial conditions, depending on the starting point of the evolution.

Let us now describe the analytic approach to the LO GLAP evolution which we apply later to the analysis of the small- $x$  HERA data. As usual, we denote as

$$\begin{aligned} q_s(n, t) &= \int_0^1 dx x^n q_s(x, t), \\ g(n, t) &= \int_0^1 dx x^n g(x, t) \end{aligned} \quad (1)$$

the moments of the quark-singlet  $q_s(x, t)$  and gluon  $g(x, t)$  distributions at a scale  $t = \ln(Q^2/\Lambda_{QCD}^2)$ . At leading order the GLAP evolution of the quark singlet distribution in terms of the initial distributions  $q_s(n, t_0)$  and  $g(n, t_0)$  has the well-known form [14]

$$\begin{aligned} q_s(n, t) &= \{(1 - h_2(n)) q_s(n, t_0) - h_1(n) g(n, t_0)\} e^{\frac{2}{\beta_0} \Lambda_+(n) \zeta} \\ &+ \{h_2(n) q_s(n, t_0) + h_1(n) g(n, t_0)\} e^{\frac{2}{\beta_0} \Lambda_-(n) \zeta}. \end{aligned} \quad (2)$$

In the above expression  $\zeta = \ln(\alpha(Q_0^2)/\alpha(Q^2))$  denotes the  $Q^2$  evolution length and  $\Lambda_{\pm}$  are the eigenvalues of the anomalous dimension matrix. The coefficients  $h_1$  and  $h_2$  may be expressed through  $\Lambda_{\pm}$  and the anomalous dimensions as

$$h_1(n) = \frac{\gamma_{qg}(n)}{\Lambda_-(n) - \Lambda_+(n)}, \quad h_2(n) = \frac{\gamma_{qq}(n) - \Lambda_+(n)}{\Lambda_-(n) - \Lambda_+(n)}, \quad (3)$$

To obtain the Bjorken- $x$  distribution from (2) one has to take the inverse Mellin transform which reads

$$x q_s(x, t) = \frac{1}{2\pi i} \int_{c-i\infty}^{c+i\infty} dn x^{-n} q_s(n, t), \quad (4)$$

where the integration contour runs to the right of all singularities of  $q_s(n, t)$ . As we shall be ultimately interested in the small- $x$  behavior of the quark distribution, let us assume that the initial conditions are given by simple poles

$$q_s(n, t_0) = \frac{A_q(t_0)}{n - \lambda_q}, \quad g(n, t_0) = \frac{A_g(t_0)}{n - \lambda_g}, \quad (5)$$

with  $1 > \lambda_{q,g} \geq 0$ . Anticipating that such a power-like rise in the initial condition is only valid for small enough  $x$ , one could introduce an additional parameter  $x_0$  above which one neglects the parton distribution and below which one assumes a power-like behavior. With this interpretation in mind it is evident that  $0 < x_0 \leq 1$ . This yields the following modified ansatz for the initial boundary,

$$q_s(n, t_0) = \frac{A_q(t_0) x_{0,q}^{-\lambda_q}}{n - \lambda_q} x_{0,q}^n, \quad g(n, t_0) = \frac{A_g(t_0) x_{0,g}^{-\lambda_g}}{n - \lambda_g} x_{0,g}^n, \quad (6)$$

where we have introduced separate  $x_0$ 's for quark and gluon distributions. As far as the magnitude of  $x_0$ 's is concerned Ref. [8] convincingly argues that  $x_{0,g}$  should be of order of 0.1.

We have found that the introduction of  $x_{0,q}$  causes problems. From a practical point of view the model parameters become highly correlated (cf. equation (6)). Secondly, the HERA data [1, 2] favor  $x_{0,q}$  to be larger than one which contradicts the interpretation of  $x_0$  as the boundary of the power-like behaviour. For these reasons we have decided to use instead the following ansatz for the initial conditions

$$q_s(n, t_0) = \frac{A_q(t_0)}{n - \lambda_q} + B_q(t_0), \quad g(n, t_0) = \frac{A_g(t_0)}{n - \lambda_g} + B_g(t_0). \quad (7)$$

The constants  $B_{q,g}$  model the leading corrections to a power-like small- $x$  boundary. Further corrections  $nB_{g,q}^{(1)}(t_0) + \dots$  can be introduced if necessary.

Our strategy for solving the Mellin inversion (4) with initial conditions (7) will be the usual one, i.e., first we close the contour in the left-half plane and then successively the residues are taken, starting from those with the largest real parts. The smaller  $x$  is, the less residues will be needed. Therefore we first discuss the poles inside the unit disc  $|n| < 1$ . Apart from the pole at  $n = \lambda$  the only other pole singularity inside the unit disc occurs at  $n = 0$ . This can be read off from the Laurent expansions of  $\Lambda_{\pm}$  and  $h_{1,2}$  which start like

$$\begin{aligned} \frac{2}{\beta_0} \Lambda_+(n) &= \frac{\tilde{a}}{n} + \Lambda_+^R(n), \\ \Lambda_+^R(n) &= -\delta_+ + \mathcal{O}(n), \\ \Lambda_-(n) &= \mathcal{O}(1), \\ h_1(n), 1 - h_2(n) &= \mathcal{O}(n), \end{aligned} \quad (8)$$

where  $\tilde{a} = 12/\beta_0$  and  $\delta_+ = (11 + 2n_f/27)/\beta_0$ . The functions  $\Lambda_+^R$ ,  $\Lambda_-$  and  $h_{1,2}$  are analytic inside the unit disc. From this one concludes that the contribution to the Mellin integral (4) from the  $\Lambda_-$ -term in (2) is just the residue of the simple pole at  $n = \lambda$

$$xq_-(x, Q^2) = A_q(t_0) h_2(\lambda_q) e^{a'\Lambda_-(\lambda_q)+b\lambda_q} + A_g(t_0) h_1(\lambda_g) e^{a'\Lambda_-(\lambda_g)+b\lambda_g}, \quad (9)$$

where  $a' = 2\zeta/\beta_0$  and  $b = \ln(\frac{1}{x})$ . The Mellin inversion of the  $\Lambda_+$ -term in (2) is complicated through the additional essential singularity at  $n = 0$ . Using that  $\Lambda_+^R$ , and  $h_{1,2}$  are analytic inside the unit disc one can formally rewrite the Mellin inversion of the  $\Lambda_+$ -term as

$$\begin{aligned} xq_+(x, Q^2) &= A_q(t_0) \hat{U}_q(\partial_b, \zeta) J(a, b; \lambda_q) + A_g(t_0) \hat{U}_g(\partial_b, \zeta) J(a, b; \lambda_g), \\ &+ \left\{ B_q(t_0) \hat{U}_q(\partial_b, \zeta) + B_g(t_0) \hat{U}_g(\partial_b, \zeta) \right\} \left( \frac{a}{b} \right)^{\frac{1}{2}} I_1(\sqrt{2ab}), \\ J(a, b; \lambda) &= \frac{1}{2\pi i} \int_{\gamma} dn \frac{e^{\frac{a}{n}+bn}}{n-\lambda} \end{aligned} \quad (10)$$

where again  $a = 12\zeta/\beta_0$ ,  $b = \ln(\frac{1}{x})$ ,  $I_1$  is the modified Bessel function [15], and  $\gamma$  surrounds both poles with positive orientation. The differential operators in (10) are constructed in such a way that their action reproduces the expansion (8), e.g.,

$$\hat{U}_g(\partial_b, \zeta) = -h_1(\partial_b) e^{\zeta\Lambda_+^R(\partial_b)}, \quad (11)$$

where  $\partial_b = \frac{\partial}{\partial b}$  denotes the derivative over the parameter  $b$ . Note, that we do not expand the initial condition around  $n = 0$ . Such an expansion would result in a term proportional to  $1/\lambda$  which diverges at  $\lambda = 0$ . It is clear that to obtain a sensible soft initial condition limit one has to keep the initial condition term as a whole.

Now, from properties of modified Bessel functions it can be shown that  $J(a, b; \lambda)$  admits the following representation

$$J(a, b; \lambda) = I_0(2\sqrt{ab}) + \frac{\lambda}{2a} e^{b\lambda} \int_0^{2\sqrt{ab}} du u e^{-\frac{\lambda}{4a}u^2} I_0(u). \quad (12)$$

In the limit  $\zeta = 0 = a$ , i.e. no  $Q^2$  evolution, the above formula exactly reproduces the corresponding initial condition.

As the next step consider the operator  $\hat{U}(\partial_b, \zeta)$ . For fixed  $\zeta$  the function  $\hat{U}(y, \zeta)$  should be looked at as a Taylor series in  $y$ . After substituting  $y$  by  $\partial_b$ , each term  $y^i$  in the above Taylor expansion becomes a differential operator that acts on  $J(a, b; \lambda)$  to give

$$J_i(a, b; \lambda) = \frac{1}{2\pi i} \int_{\gamma} dn n^i \frac{e^{\frac{a}{n}+bn}}{n-\lambda}. \quad (13)$$

Again, the above integral can be evaluated to give

$$J_i(a, b; \lambda) = \lambda^i \sum_{k=0}^i \left( \frac{n_0}{\lambda} \right)^k I_k(2\sqrt{ab}) + \frac{\lambda^{i+1}}{2a} e^{b\lambda} \int_0^{2\sqrt{ab}} du u e^{-\frac{\lambda}{4a}u^2} I_0(u), \quad (14)$$

where  $n_0 = \sqrt{\frac{a}{b}}$ . For a soft boundary  $J_i(a, b; \lambda = 0)$  simplifies to

$$J_i(a, b; \lambda = 0) = n_0^i I_i(2\sqrt{ab}). \quad (15)$$

Combining the representation

$$I_k(z) = \frac{1}{\pi} \int_0^\pi dt e^{z \cos t} \cos(kt) \quad (16)$$

with the Taylor expansion of  $\hat{U}(\partial_b, \zeta)$  it is possible first to compute the geometric sums over  $i$  in (13) and then to evaluate their infinite series by a single complex integral. One obtains

$$\begin{aligned} xq_+(x, t) &= A_q(t_0) \lambda_q U_q(\lambda_q, \zeta) \frac{e^{b\lambda_q}}{2a} \int_0^{2\sqrt{ab}} du u e^{-\frac{\lambda_q}{4a} u^2} I_0(u) \\ &+ A_g(t_0) \lambda_g U_g(\lambda_g, \zeta) \frac{e^{b\lambda_g}}{2a} \int_0^{2\sqrt{ab}} du u e^{-\frac{\lambda_g}{4a} u^2} I_0(u) \\ &+ \frac{1}{\pi} \int_0^\pi dt e^{2\sqrt{ab} \cos t} \text{Re} \left( \frac{A_q(t_0) \lambda_q U_q(\lambda_q, \zeta)}{\lambda_q - n_0 e^{it}} + \frac{A_g(t_0) \lambda_g U_g(\lambda_g, \zeta)}{\lambda_g - n_0 e^{it}} \right) \\ &- \frac{n_0}{\pi} \int_0^\pi dt e^{2\sqrt{ab} \cos t} \text{Re} \left( \frac{A_q(t_0) U_q(n_0 e^{it}, \zeta) e^{it}}{\lambda_q - n_0 e^{it}} + \frac{A_g(t_0) U_g(n_0 e^{it}, \zeta) e^{it}}{\lambda_g - n_0 e^{it}} \right) \\ &+ \frac{n_0}{\pi} \int_0^\pi dt e^{2\sqrt{ab} \cos t} \text{Re} \left\{ B_q(t_0) U_q(n_0 e^{it}, \zeta) + B_g(t_0) U_g(n_0 e^{it}, \zeta) \right\}, \quad (17) \end{aligned}$$

where  $\text{Re}$  denotes the real part. This formula is valid if  $U(z, \zeta)$  admits a Taylor expansion around  $z = 0$  along the integration contours  $z = n_0 \exp(it)$ . Thus, because the convergence radius of  $U_{g,q}(z, \zeta)$  is the unit disc, only data with  $n_0 < 1$  should be compared with (17) which is not a severe restriction in practice [13]. Of course the same restriction also applies to approximations that are constructed from (14), i.e. where only a finite number of terms are taken into account. The formula (17) looks more complicated than it really is, although it is necessary to take care about a proper definition of the multi-valued complex square root used in the definition of the anomalous dimension along the contour of integration. In the soft boundary limit the first two terms in (17) vanish and the last term simplifies somewhat. Apart from the kinematical restriction  $n_0 < 1$ , equation (17) together with (9) yield the exact contribution to the parton radiation arising from the leading singularity at  $n = 0$  of the anomalous dimensions and the leading pole at  $n = \lambda$  of the boundary.

The next singularity in the Mellin plane at  $n = -1$  can be treated along the same lines that lead to (17) but gives only a numerically small correction at small  $x$  because of an extra factor  $x$  that multiplies most terms. An important difference now is the absence of a simple pole like the one at  $n = \lambda$  above. It can explicitly be shown that this causes all contributions from the  $n = -1$  singularity to vanish in the no-evolution limit as it should, because the initial boundary is already recovered by the leading poles at  $n = \lambda$  and  $n = 0$ . Therefore one can expect that for moderate  $Q^2$  this term is additionally suppressed. In

principle it is an easy task to incorporate effects from the pole at  $n = -1$  but for consistency one should then also include the next pole from the initial conditions. Rather than to proceed this way we neglect all poles with  $Re(n) \leq -1$  and check the quality of the approximation a posteriori by comparing with the exact result. Figure 1 shows such a comparison with the exact LO CTEQ [5] at  $Q^2 = 10 \text{ GeV}$ . The approximation (7) to the initial conditions has been determined from the CTEQ input parameterizations. For  $q_-$  we use equation (9) and  $q_+$  is constructed by taking in (14) the first non-vanishing term in the expansion of  $U_{q,g}(y, \zeta)$  around  $y = 0$ . One learns from this figure that when keeping only data with, say,  $x \leq 5 \cdot 10^{-3}$ , it is certainly justified to neglect poles with  $Re(n) \leq -1$ . Further, despite the fact that typically  $n_0$  is not particularly small [13], it is not necessary to evaluate the resummed formula (17) but it is sufficient to take just the first term from the expansions that are generated by (14), i.e.

$$\begin{aligned}
xq_s(x, t) = & \left[ (0.198 A_q(t_0) + 0.444 A_g(t_0)) \left(\frac{a}{b}\right)^{\frac{1}{2}} I_1(2\sqrt{ab}) \right. \\
& + (0.198 \lambda_q A_q(t_0) + 0.444 \lambda_g A_g(t_0)) I_0(2\sqrt{ab}) \\
& \left. + (0.198 B_q(t_0) + 0.444 B_g(t_0)) \left(\frac{a}{b}\right) I_2(2\sqrt{ab}) \right] e^{-\delta+\zeta} \\
& + \left[ 0.198 A_q(t_0) \frac{\lambda_q^2}{2a} x^{-\lambda_q} \int_0^{2\sqrt{ab}} du u e^{-\frac{\lambda_q}{4a} u^2} I_0(u) \right. \\
& \left. + 0.444 A_g(t_0) \frac{\lambda_g^2}{2a} x^{-\lambda_g} \int_0^{2\sqrt{ab}} du u e^{-\frac{\lambda_g}{4a} u^2} I_0(u) \right] e^{-\delta+\zeta} \\
& + \left[ (1 - 0.198\lambda_q) A_q(t_0) x^{-\lambda_q} - 0.444 \lambda_g A_g(t_0) x^{-\lambda_g} \right] e^{-\frac{\zeta}{\beta_0} 1.185 \zeta}. \quad (18)
\end{aligned}$$

This is largely due to the fact that the Taylor coefficients that multiply these terms are rather small for sub-leading terms and values of  $\zeta$  typical for the current data. Note, that the extreme case where only the first non-vanishing term in the expansion of  $U_{q,g}$  is kept and  $\lambda_q, \lambda_g$  are set to zero corresponds to the soft boundary solution that has been obtained in [8] by means of a saddle-point approximation for large  $\zeta$  and large  $\xi$ .

Furthermore we compare in Figure 1 our expansion scheme with a naive pole approximation which takes into account the residue of the rightmost pole in Mellin space at  $n = \lambda_q, \lambda_g$  only. A priori we expect such an expansion scheme to work in the regime of large  $\lambda$ , where the pole is sufficiently separated from the essential singularity at  $n = 0$  arising from the anomalous dimensions. Already for  $\lambda$  values around  $0.2 - 0.3$  as represented by the CTEQ parameters (see Table 1) the difference between exact and approximated solution becomes larger than the experimental errors. In case of yet smaller  $\lambda$  we have checked that the discrepancy strongly increases. Thus the naive pole approximation has to be replaced by the more accurate formula, like equation (18), in a data analysis where  $\lambda$  is a variable fit parameter.

Using the above considerations we have performed a fit [16] to the HERA data [1, 2] with the formula (18), starting from scales  $Q_0^2 = 1$  and  $2.56 \text{ GeV}^2$ , the latter scale corresponding to the CTEQ starting point. In both fits the number of quark flavors was

globally assumed to be  $n_f = 4$ . The results are shown in Table 1. For orientation, the table contains also the corresponding fit parameters determined from the CTEQ initial conditions. As far as the fit with the starting point  $Q_0^2 = 2.56 \text{ GeV}^2$  is considered, the parameters  $A_q$  and  $A_g$  as well as the slopes  $\lambda_g$  and  $\lambda_q$  agree well with what has been found in [5] from a global fit. It demonstrates the self-consistency of the GLAP evolution in the small- $x$  region: the parameters of the fit which determine the leading small- $x$  behavior are indeed determined mainly by the small- $x$  data. At the same time if one is interested only in the QCD description of the small- $x$  data it is legitimate to use the analytical approximation to the GLAP evolution, saving much effort as compared with a global fitting procedure. The parameters  $B_q$  and  $B_g$  are reproduced less accurately, but still the present fit seems to reproduce their correct signs. Note, that  $B_q$  comes out from both the CTEQ and our fits greater than zero which contradicts the interpretation  $x_{0,q}$ , as we have discussed above. The relatively large errors are due to the fact that  $B_q(t_0)$  and  $B_g(t_0)$  generate non-leading contributions at small- $x$  and therefore are less sensitive to the data in this region.

The fit with a low starting point of  $Q_0^2 = 1 \text{ GeV}^2$  results with the same data being parameterized by a soft gluon boundary, although the corresponding  $\lambda_g$  parameter is hardly constrained by the fit. It means that for a sufficiently large evolution length soft and hard boundaries result in a similar shape of  $F_2(x, Q^2)$  at small- $x$ . Note, that although equation (18) describes asymptotic behavior of the evolution starting from a hard boundary, the first three terms on the right-hand side have a non power-like, i.e. soft, small- $x$  behavior. To illustrate this point we show in Figure 2 various contributions to  $F_2(x, Q^2)$  for  $Q^2 = 10$  and  $1000 \text{ GeV}^2$ , respectively, as determined by our fit with the starting scale  $Q_0^2 = 2.56 \text{ GeV}^2$ . As already stated in [13] it is important to include  $q_-(x, Q^2)$  in an analysis including data in a moderate  $Q^2$  range. This contribution is represented by the last term in Eq.(18). For large  $Q^2$  this part of the solution gets strongly suppressed as expected from the very beginning. On the other hand the soft part, identified as the first three terms on the right-hand side of equation (18), has a shape which is similar to the full solution. In other words, in the  $x$  domain covered by the current experiments soft and power-like initial conditions can be indistinguishable. This observation may help to understand the known fact that the global fits can explain the data equally well starting from soft [6] or hard [7] initial conditions.

Keeping  $\lambda_g$  and  $\lambda_q$  equal to zero, and allowing for the starting point of the evolution to be as low as  $0.45 \text{ GeV}^2$ , we have obtained the fit presented in the last row in Table 1. It is consistent with results of [6] where the LO fit starting from a yet lower scale  $0.24 \text{ GeV}^2$  and valence-like distributions with  $\lambda_g, \lambda_q < 0$  was presented, but one should keep in mind that the approximation (18) does not describe the GLAP evolution from such initial conditions with a sufficient accuracy.

Finally we have investigated the double asymptotic scaling behavior of  $F_2$  as function of the scaling variables  $\rho = \sqrt{\xi/\zeta}$ ,  $\sigma = \sqrt{\xi\zeta}$  ( $\xi = \ln(1/x)$ ,  $\zeta = \ln \frac{\alpha_s(Q_0^2)}{\alpha_s(Q^2)}$ ), as advocated in [8]. After rescaling  $F_2$  by the factor

$$R_F = N_F \rho \sqrt{\sigma} \exp(-2\gamma\sigma + \delta_+ \sigma/\rho) \quad (19)$$

Data range	$Q_0^2$	$A_g(t_0)/A_q(t_0)$	$B_g(t_0)/B_q(t_0)$	$\lambda_g/\lambda_q$	$\chi^2/\text{d.o.f.}$
$x < 0.005,$ $Q^2 > 3\text{GeV}^2$	2.56 GeV <sup>2</sup> (fixed)	0.84±0.08, 0.57±0.03	-0.81±1.02, 1.21 ±2.33	0.27±0.02, 0.18±0.01	0.78
CTEQ [5]	2.56 GeV <sup>2</sup> (fixed)	0.854, 0.502	-2.693, 1.799	0.305, 0.200	
$x < 0.005,$ $Q^2 > 3\text{GeV}^2$	1.0 GeV <sup>2</sup> (fixed)	0.19±0.05, 0.70±0.03	-1.62±0.49, 6.27 ±0.77	0.32±0.03, 0.11±0.01	0.78
$x < 0.005,$ $Q^2 > 3\text{GeV}^2$	0.45 ± 0.01 GeV <sup>2</sup>	0.00±0.06, 1.04±0.04	0.00±0.17, 1.61 ±0.29	0.00 (fixed), 0.00 (fixed)	0.87

Table 1: Results of the fit of equation (18) to the small- $x$  HERA data [1, 2]. For orientation, the table contains also the corresponding fit parameters determined from the results of the CTEQ LO global fit [5]. In the last row we have kept  $\lambda_g$  and  $\lambda_q$  equal to zero and allowed for perhaps unphysically low starting point  $Q_0^2$  in order to present a fit with soft initial conditions for both quark and gluon distributions. All errors are parabolic, see [16] for details.

where  $\delta_+ = (11 + \frac{2}{27}n_f)/\beta_0$ , we observe in Figure 3 that the data accumulate in a flat area in the  $\rho$ - $\sigma$ -plane, despite the fact that the plot corresponds to a power-like initial quark distribution at  $Q_0^2 = 1 \text{ GeV}^2$ . In other words, the kinematic bounds of current experiments restrict the position of the data points to a domain in the  $\rho$ - $\sigma$ -plane, in which  $R_F F_2$  hardly differs from a flat plane. On the other hand, the double-asymptotic scaling interpretation does not hold anymore if the starting point is taken to be  $Q_0^2 = 2.56 \text{ GeV}^2$  [17], mainly due to the redefinition of the  $Q^2$  evolution length  $\zeta$ , see Figure 4.

In summary, we have presented an approximation scheme for solving analytically the GLAP evolution at small  $x$  that treats corrections to the strict small- $x$  limit in a systematic way. In contrast to saddle-point approximations there is no need to have  $Q^2$  very large. Our solution interpolates smoothly between soft and hard boundaries. For moderately hard boundaries we have found that the pole approximation alone is not sufficient to adequately reproduce the full QCD evolution. The fit shows that it is not necessary to perform a global analysis in the full Bjorken- $x$  range if one is interested only in the parameters which determine the small- $x$  behavior of parton distributions at the initial scale. We have confirmed the wisdom arising from the global fits, that the slopes of initial quark and gluon distributions depend critically on the starting point of the evolution. The same HERA data can be described by either a hard boundary at  $Q^2 = 2.56 \text{ GeV}^2$  or a soft one if the starting point is lowered below  $Q^2 = 1.0 \text{ GeV}^2$ . The interpretation of the current data in terms of double asymptotic scaling crucially depends on the magnitude of the starting point of the  $Q^2$  evolution.



### **Acknowledgments**

A.S. thanks Prof. J. Kwieciński for useful discussions. This work was supported in part by BMBF, KBN grant 2 P03B 065 10 and German-Polish exchange program X081.91.

## References

- [1] ZEUS Collaboration, M. Derrick et al., *Z. Phys.* **C69**, 607 (1996).  
ZEUS Collaboration, M. Derrick et al., *Measurement of the  $F_2$  structure function in deep inelastic  $e^+p$  scattering using 1994 data from the ZEUS detector at HERA*, DESY-96-076, hep-ex/9607002 (1996)
- [2] H1 Collaboration, S. Aid et al., *Nucl. Phys.* **B470**, 3 (1996).
- [3] We cannot possibly do the justice here to all papers which have been published recently. For some recent reviews see e.g.,  
J. Kwieciński, *Acta Phys. Polon.* **B26**, 1933 (1995); **B27**, 893 (1996);  
J. Blümlein, T. Doyle, F. Hautmann, M. Klein, A. Vogt, *Structure functions in deep inelastic scattering at HERA*, hep-ph/9609425, to be published in the proceedings of Workshop on Future Physics at HERA;  
L.N. Lipatov, *Small  $x$  physics in perturbative QCD*, DESY-96-132, hep-ph/9610276, (1996).
- [4] CTEQ collaboration, H. L. Lai et al., *Phys. Rev.* **D51**, 4763, (1995);  
CTEQ collaboration, H. L. Lai et al., *Improved parton distributions from global analysis of recent deep inelastic scattering and inclusive jet data*, hep-ph/9606399 (1996).
- [5] CTEQ collaboration, H. L. Lai et al., *Improved parton distributions from global analysis of recent deep inelastic scattering and inclusive jet data*, hep-ph/9606399 (1996).
- [6] M. Glück, E. Reya, A. Vogt, *Zeit.Phys.* **C67**, 433 (1995).
- [7] A. D. Martin, R. G. Roberts and W. J. Stirling, *Phys. Rev.* **D50**, 6734, (1994).
- [8] A.DeRujula et al., *Phys. Rev.* **D10** 1649 (1974);  
S. Forte and R. Ball, *Phys.Lett.* **B335**, 77 (1994);  
S. Forte and R. Ball, *Universality and Scaling in Perturbative QCD at Small  $x$* , *Acta Phys. Polon.* **B26**, 2097, (1995);  
S. Forte and R. Ball, *Double Asymptotic Scaling '96*, hep-ph/9610268 (1996).
- [9] G.M. Frichter, D.W. McKay and J.P. Ralston, *Phys. Rev. Lett.* **74**, 1508 (1995).
- [10] A.V. Kotikov, *Small  $x$  behavior of parton distributions in the proton*, hep-ph/9504357 (1995).
- [11] F.J. Yndurain, *On the theoretical analysis of the small  $x$  data in recent HERA papers*, FTUAM-96-19, hep-ph/9605265 (1996);  
K. Adel, F. Barreiro, F.J. Yndurain, *Theory of small  $x$  deep inelastic scattering: NLO evaluations*, FTUAM-96-39, hep-ph/9610380 (1996);  
C. Lopez, F. Barreiro, F.J. Yndurain, *NLO predictions for the growth of  $F_2$  at small  $x$  and comparison with experimental data*, DESY-96-087, hep-ph/9605395 (1996).

- [12] T. Gehrmann and W.J. Stirling, Phys. Lett. **B365**, 347(1996).
- [13] L. Mankiewicz, A. Saalfeld and T. Weigl, *On the analytical approximation to the GLAP evolution at small  $x$  and moderate  $Q^2$* , hep-ph/9612297 (1996).
- [14] R. G. Roberts, *The structure of the proton*. Cambridge University Press, Cambridge (1990).
- [15] M. Abramowitz and I.A. Stegun, “Handbook of Mathematical Functions”, Dover Publications Inc., New York, 1970.
- [16] F. James, *MINUIT - Function Minimization and Error Analysis*, CERN Program Library Entry **D506**.
- [17] J.R. Forshaw, R.G. Roberts, Phys. Lett. **B351**, 308 (1995).

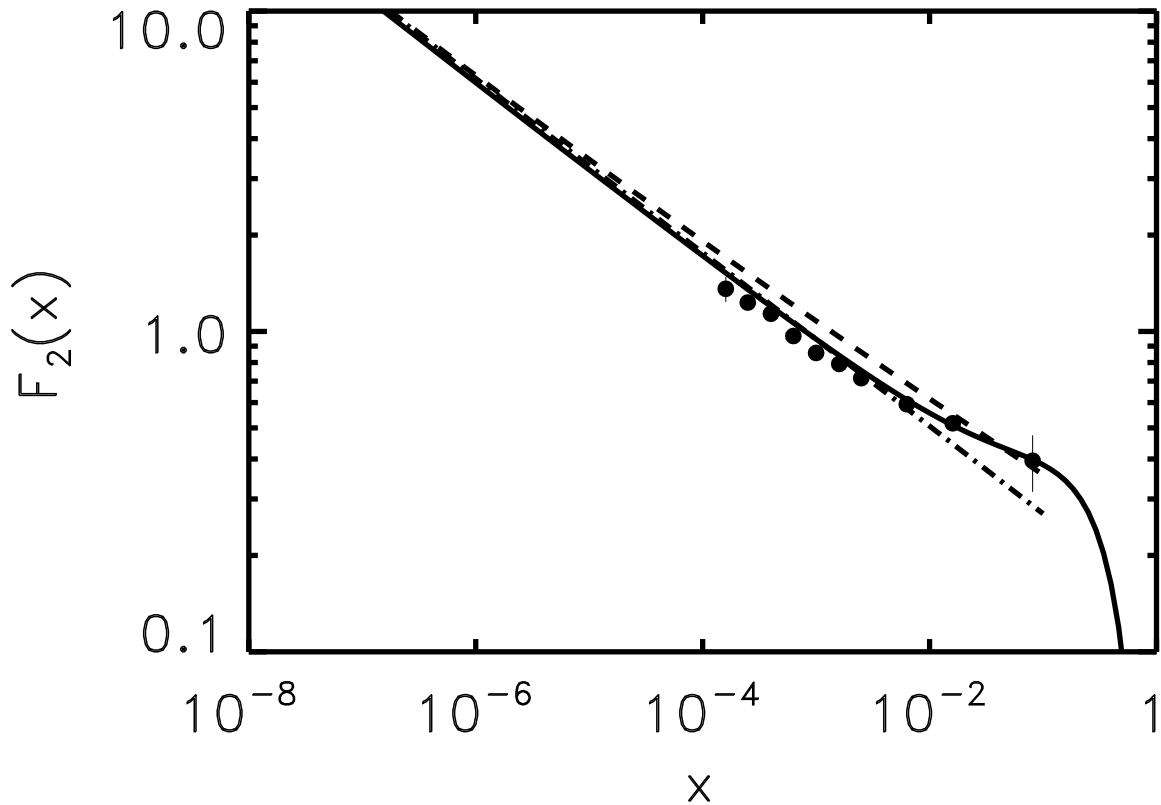


**Fig. 1** Comparison of the full (solid line) and the approximate evolution according to equation (18) (dot-dashed line) at  $Q^2 = 10 \text{ GeV}^2$ . The initial conditions at  $Q^2 = 2.56 \text{ GeV}^2$  correspond to the CTEQ4L fit [5]. The dashed line shows the result of the naive pole approximation, based on taking into account the residue of the rightmost pole in the Mellin plane only. Data points [1] correspond to  $Q^2 = 10 \text{ GeV}^2$ .

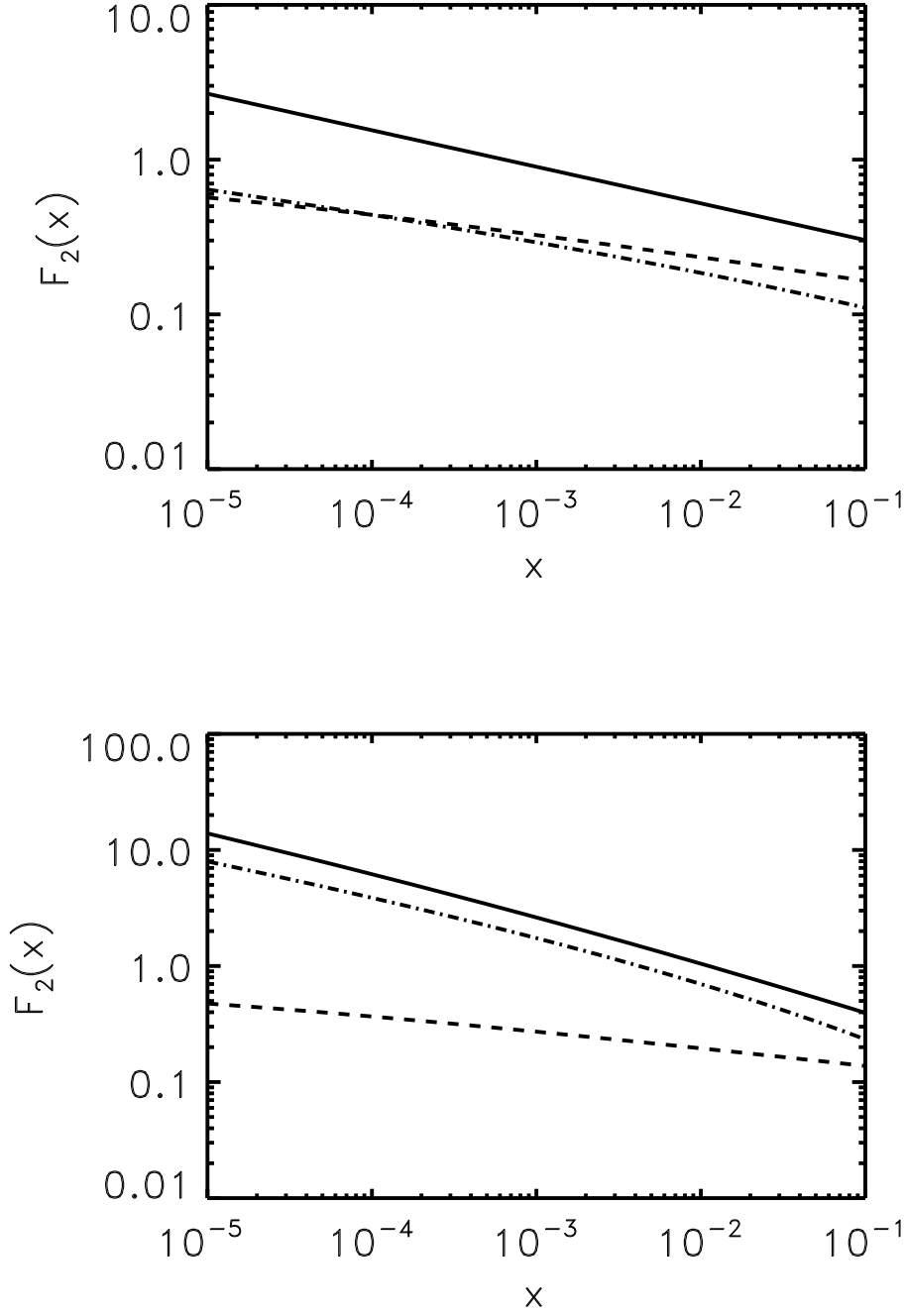


**Fig. 2** Contributions of soft terms, and small eigenvalue  $5/18q_-(x, Q^2)$  terms to  $F_2(x, Q^2)$  at  $Q^2 = 10 \text{ GeV}^2$  (upper plot) and  $Q^2 = 1000 \text{ GeV}^2$  (lower plot), as obtained from our fit with the starting scale  $Q_0^2 = 2.56 \text{ GeV}^2$ . Full lines represent  $F_2(x, Q^2)$ . Dot-dashed lines show the soft contribution, as given by the first three terms on the right-hand side of equation (18). Dashed lines show the small eigenvalue contribution  $5/18q_-(x, Q^2)$ .

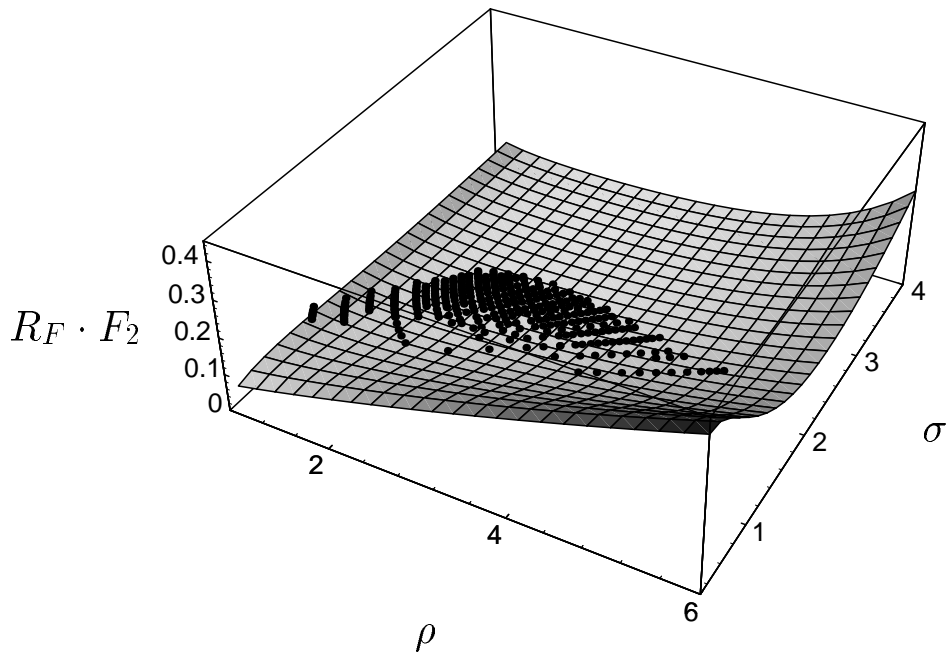


**Fig. 3**  $R_F F_2$  as a function of the scaling variables  $\rho$  and  $\sigma$  as given by the fit with  $Q_0^2 = 1.0 \text{ GeV}^2$ . Dots denote data points [1, 2] with  $Q^2 \geq 3 \text{ GeV}^2$ . Note that the small- $x$  region corresponds to large values of  $\rho$ .

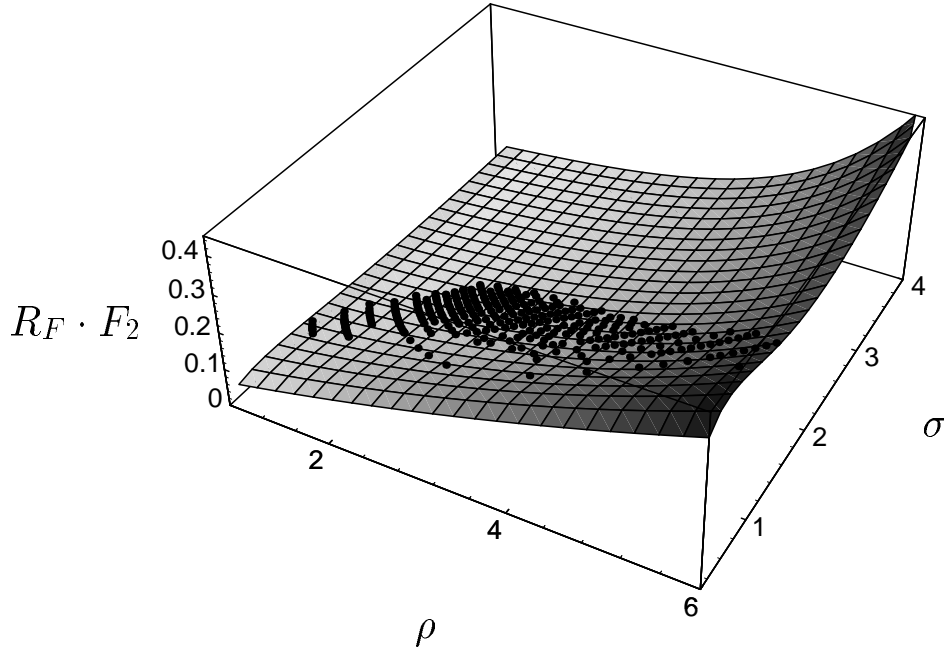


**Fig. 4**  $R_F F_2$  as a function of the scaling variables  $\rho$  and  $\sigma$  as given by the fit with  $Q_0^2 = 2.56 \text{ GeV}^2$ . Dots again denote data points [1, 2] with  $Q^2 \geq 3 \text{ GeV}^2$ . The  $R_F F_2(\rho, \sigma)$  surface is not flat and the double-asymptotic scaling interpretation does not hold anymore.